MOLECULAR AND CELLULAR BIOLOGY, Apr. 1991, p. 2040–2048
0270-7306/91/042040-09$02.00/0

Vol. 11, No. 4

The *erb*B-2 Mitogenic Signaling Pathway: Tyrosine Phosphorylation of Phospholipase C-γ and GTPase-Activating Protein Does Not Correlate with *erb*B-2 Mitogenic Potency

FRANCESCA FAZIOLI,[1] UH-HYUN KIM,[2] SUE GOO RHEE,[2] CHRISTOPHER J. MOLLOY,[1] ORESTE SEGATTO,[1] AND PIER PAOLO DI FIORE[1]*

Laboratory of Molecular and Cellular Biology, National Cancer Institute,[1] and Laboratory of Biochemistry, National Heart, Lung and Blood Institute,[2] National Institutes of Health, Bethesda, Maryland 20892

Received 28 August 1990/Accepted 15 January 1991

The *erb*B-2 gene product, gp185^{erbB-2}, unlike the structurally related epidermal growth factor (EGF) receptor (EGFR), exhibits constitutive kinase and transforming activity. We used a chimeric EGFR/*erb*B-2 expression vector to compare the mitogenic signaling pathway of the *erb*B-2 kinase with that of the EGFR, at similar levels of expression, in response to EGF stimulation. The EGFR/*erb*B-2 chimera was significantly more active in inducing DNA synthesis than the EGFR when either was expressed in NIH 3T3 cells. Analysis of biochemical pathways implicated in signal transduction by growth factor receptors indicated that both phospholipase C type γ (PLC-γ) and the p21^{ras} GTPase-activating protein (GAP) are substrates for the *erb*B-2 kinase in NIH 3T3 fibroblasts. However, under conditions in which activation of the *erb*B-2 kinase induced DNA synthesis at least fivefold more efficiently than the EGFR, the levels of *erb*B-2- or EGFR-induced tyrosine phosphorylation of PLC-γ and GAP were comparable. In addition, the stoichiometry of tyrosine phosphorylation of these putative substrates by *erb*B-2 appeared to be at least an order of magnitude lower than that induced by platelet-derived growth factor receptors at comparable levels of mitogenic potency. Thus, our results indicate that differences in tyrosine phosphorylation of PLC-γ and GAP do not account for the differences in mitogenic activity of the *erb*B-2 kinase compared with either the EGFR or platelet-derived growth factor receptor in NIH 3T3 fibroblasts.

The *erb*B-2 gene encodes a growth factor receptor-like protein (1, 3), gp185^{erbB-2}, which has extensive structural and sequence homologies with the epidermal growth factor (EGF) receptor (EGFR) (37). These similarities have prompted comparative studies of their biological actions. We have previously demonstrated that gp185^{erbB-2} and EGFR exhibit cell-specific differences in their ability to couple with mitogenic signaling pathways. In particular, gp185^{erbB-2} is highly transforming when expressed in NIH 3T3 fibroblasts but a poor transducer of a mitogenic signal in the 32D hematopoietic line (5, 7). Conversely, the EGFR was able to deliver a potent mitogenic signal in this latter cell line but transformed NIH 3T3 cells 100-fold less efficiently than gp185^{erbB-2} (4, 7, 26). These results strongly argue that the mitogenic pathways activated by these two kinases must be different, at least in part.

Efforts to characterize the biochemical events triggered by activation of the *erb*B-2 tyrosine kinase in comparison to the EGFR have been hampered by lack of a ligand for gp185^{erbB-2}. Moreover, in contrast to the EGFR, gp185^{erbB-2} displays constitutive kinase and transforming activities (7, 30, 31, 34). A strategy to circumvent these problems derives from the engineering of chimeric molecules containing the extracellular domain of the EGFR and the intracytoplasmic region of gp185^{erbB-2} (EGFR/*erb*B-2 chimera). Such an approach has been used successfully by Lee et al. (15) and Lehväslaiho et al. (16), who have reported that an EGFR/*erb*B-2 chimera is more stringently regulated in terms of kinase activity than the parental gp185^{erbB-2} and is capable of transducing a mitogenic signal upon EGF binding.

At least two major pathways have been implicated in the transduction of the mitogenic signal by tyrosine kinase growth factor receptors, one leading to increased phosphatidylinositol 4,5-bisphosphate (PIP_2) breakdown and one involving signaling through the p21^{ras}/GTPase-activating protein (GAP) system. Evidence for the relevance of these two pathways in the regulation of cell proliferation has been gathered by a variety of approaches, including microinjection of purified proteins and neutralizing antibodies (23, 32, 33). A direct biochemical link between the activation of growth factor receptor kinases and these two systems has been provided by evidence that both phospholipase C type γ (PLC-γ), a key enzyme in the phosphoinositide breakdown pathway, and GAP are directly phosphorylated on tyrosine residues by the platelet-derived growth factor (PDGF) receptor (PDGFR) and EGFR (9, 12, 17–19, 39, 40).

In the present study, we engineered a chimeric EGFR/*erb*B-2 molecule to study *erb*B-2 mitogenic action and signaling pathways in comparison to the EGFR. Our results show that coupling with pathways other than those activated by PLC-γ and GAP tyrosine phosphorylation must be responsible for the differences in mitogenic potencies between *erb*B-2 and EGFR expressed at the same levels in a fibroblast target cell.

MATERIALS AND METHODS

Transfection assays. DNA transfection was performed by the calcium phosphate precipitation technique (10, 41). Transforming efficiency was calculated as described previously (6). Cells expressing the Eco*gpt* gene were selected for their ability to form colonies in mycophenolic acid-containing medium (24). The [^{3}H]thymidine incorporation assay was

* Corresponding author.

performed as described previously (4). EGF and PDGF-BB were purchased from Collaborative Research and Amgen, respectively.

Eukaryotic expression vectors. The long terminal repeat (LTR)-*erb*B-2 (5) and LTR-EGFR (4) expression vectors have been described previously. The LTR-EGFR/*erb*B-2 expression vector was engineered starting from modified versions of LTR-*erb*B-2 and LTR-EGFR plasmids in which a novel *Cla*I site had been engineered in homologous positions in the sequences of *erb*B-2 and EGFR immediately preceding the transmembrane region, and its construction is described in detail elsewhere (16a). Briefly, the novel *Cla*I site and an *Mlu*I site located in the LTR-based (4, 5, 7) vectors downstream of the natural stop codons of the *erb*B-2 and EGFR cDNAs were used to substitute the sequence encoding the *erb*B-2 transmembrane and intracellular domains for the analogous sequence of EGFR. This recombination yielded the LTR-EGFR/*erb*B-2 expression vector. The resulting EGFR/*erb*B-2 chimera contained the entire extracellular domain of the EGFR (amino acid residues −24 to 621 of the original EGFR sequence [37]), whereas the transmembrane and intracellular portions derived from *erb*B-2 (amino acid residues 654 to 1255 of the original *erb*B-2 sequence [3]). The LTR-EGFR/*erb*B-2 vector was sequenced in both strands of the regions which underwent genetic manipulation to verify that the predicted structures were achieved after the recombination procedures.

Protein analysis. Cells grown to subconfluence were incubated overnight in serum-free medium supplemented with transferrin (5 μg/ml) and selenium (10 nM) and then exposed to growth factors at the indicated concentrations for the indicated lengths of time at 37°C (see figure legends). Lysis was performed in a buffer containing 1% Triton X-100, 50 mM HEPES (*N*-2-hydroxyethylpiperazine-*N'*-2-ethanesulfonic acid, pH 7.5), 150 mM NaCl, 10% glycerol, 1.5 mM $MgCl_2$, 5 mM EGTA (ethylene glycol tetraacetic acid), 5 mM sodium orthovanadate, 2 mM phenylmethylsulfonyl fluoride, 50 μg of aprotinin per ml, and 10 mM $NaPP_i$. Immunoprecipitation and immunoblot analysis were performed as described previously (4, 6). The antibodies used were a mixture of six monoclonal antibodies (MAbs) directed against PLC-γ (35) and rabbit antipeptide polyclonal sera against *erb*B-2 (M1 and M6 sera [6]), EGFR (E7 serum [6]), and GAP (637 serum; a kind gift of M. Marshal, Merck Sharp & Dohme Research Laboratories). Three antiphosphotyrosine (anti-PTyr) antibodies were also used: an affinity-purified polyclonal serum prepared by the method of Pang et al. (25) and two commercially available MAbs (MAb PY20 [ICN] and an anti-PTyr MAb [UBI]). The results presented in this article were obtained with the affinity-purified polyclonal antibody; similar results were, however, obtained with both the commercially available MAbs.

The specificity of immunodetection for the peptide antisera was controlled by performing parallel staining of identical blots with antibodies preabsorbed with the specific peptides (1 mg/ml) (data not shown). In the case of the anti-PTyr antibody, specificity was controlled by preabsorption of the antibody with either PTyr, phosphoserine, or phosphothreonine (data not shown).

Analysis of inositol phosphates. Cells were prelabeled with 20 μCi of [*myo*-2-^{3}H]inositol (15 Ci/mmol; New England Nuclear) per dish for 48 h. Monolayers were treated in serum-free medium for 4 h and then stimulated with EGF (100 ng/ml) or PDGF (100 ng/ml) in the presence of 20 mM lithium cloride. The reaction was stopped 30 min later, and ^{3}H-inositol phosphates were analyzed as described before (29).

Tryptic phosphopeptide mapping. Phosphorylated PLC-γ bands were cut from the gel, ground in 0.05 M NH_4HCO_3 in 1.5-ml microfuge tubes with a Kontes pellet pestle motor, extracted, and subjected to tryptic digestion as described elsewhere (11). The resultant phosphopeptides were separated in two dimensions on 100-μm thin-layer cellulose plates (EM Science) by electrophoresis at pH 1.9 in acetic acid–88% formic acid–water (156:50:1,794, vol/vol) for 30 min at 1 kV, followed by chromatography in *n*-butanol–pyridine–acetic acid–water (75:50:15:60, vol/vol). Thin-layer electrophoresis was performed on a Hunter thin-layer peptide mapping system (CBS Scientific Co.).

RESULTS

An EGFR/*erb*B-2 chimeric molecule is more efficient than the EGFR as a mitogenic signal transducer in NIH 3T3 cells. In order to test the biological activity of the *erb*B-2 kinase under conditions of controlled ligand-induced activation, we engineered an EGFR/*erb*B-2 chimeric molecule possessing the extracellular domain of EGFR and the intracellular domain of *erb*B-2 (see Materials and Methods and Fig. 1A). The EGFR/*erb*B-2 expression vector was transfected into NIH 3T3 cells. For comparison, we transfected the same cells with the LTR-*erb*B-2 (5) and LTR-EGFR (4) expression vectors. As reported previously (4, 7), *erb*B-2 acted as a potent oncogene, inducing about 10^4 transformed foci (FFU) per pmol of added DNA (Fig. 1A). In contrast, EGFR transforming ability was strictly dependent upon addition of EGF to the culture medium. Even under these conditions, its transforming activity was 100-fold lower than that of *erb*B-2 (Fig. 1A). As shown in Fig. 1A, the EGFR/*erb*B-2 chimera displayed a low but reproducibly detectable level of transforming activity in the absence of EGF. However, upon EGF addition, its transforming activity increased strikingly to about 10^4 FFU/pmol of DNA. Thus, under conditions of ligand stimulation, the EGFR/*erb*B-2 chimera displayed *erb*B-2-like transforming efficiency (Fig. 1A).

To compare the signaling properties of the *erb*B-2 and EGFR kinases, we used two marker-selected mass cell populations, NIH-EGFR/*erb*B-2 and NIH-EGFR, displaying a comparable number of EGF-binding sites (approximately 1.5×10^6 binding sites per cell; see legend to Fig. 1B for details). Figure 1B shows the EGF dose-response profiles of these two cell lines in a representative [^{3}H]thymidine incorporation assay. While both cell lines exhibited a similar 50% effective dose (ED_{50}) for EGF (60 to 80 pM), NIH-EGFR cells showed a maximal biological response which was only 20% of that observed with NIH-EGFR/*erb*B-2. Similar results were obtained when mass cell populations expressing lower receptor numbers (about 2.0×10^5 to 3.0×10^5 receptors per cell) were used and when the EGFR and EGFR/*erb*B-2 constructs were expressed in NR6 cells, which are devoid of endogenous EGFR (data not shown). As a control, we tested the ability of NIH-EGFR/*erb*B-2 and NIH-EGFR to respond to PDGF-BB homodimers. [^{125}I]PDGF-BB binding experiments revealed about 1.3×10^5 PDGFRs per cell for each cell line. As evident in Fig. 1C, the two cell lines displayed comparable responses to PDGF-BB. All of these results taken together show that the *erb*B-2 kinase delivers a more potent mitogenic signal than the EGFR kinase under identical conditions of ligand activation.

***erb*B-2 kinase induces tyrosine phosphorylation of a different subset of cellular proteins than either EGFR or**

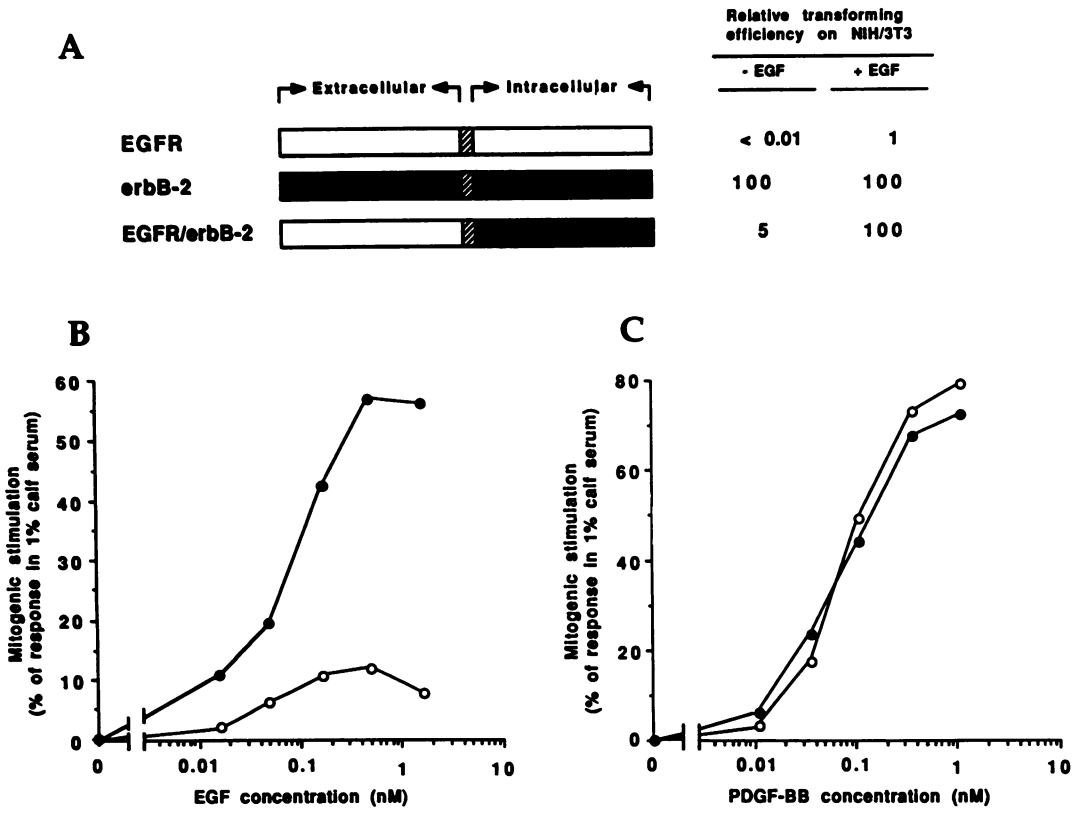

FIG. 1. Characterization of the EGFR/*erb*B-2 chimera in comparison with wild-type EGFR and *erb*B-2. (A) Transforming activity. The LTR-EGFR, LTR-*erb*B-2, and LTR-EGFR/*erb*B-2 expression vectors were transfected into NIH 3T3 cells as described previously (6). Assays were scored at 3 weeks. Where indicated, EGF (20 ng/ml) was added to the culture medium at day 14, and assays were scored a week later. Transforming efficiency was calculated in focus-forming units per picomole of added DNA, after normalization for the efficiency of colony formation in parallel dishes treated with mycophenolic acid-containing medium. Results are expressed as a fraction of the transforming efficiency of LTR-EGFR in the presence of EGF (which is defined as 1). Under our conditions of analysis, we typically obtained about 10^2 FFU/pmol of DNA (normalized to 10^4 mycophenolic acid-resistant colonies per pmol of DNA) for the LTR-EGFR in the presence of EGF. The transforming efficiency of LTR-*erb*B-2 was about 10^4 FFU/pmol (for 10^4 mycophenolic acid-resistant colonies per pmol). The LTR-EGFR/*erb*B-2 chimeric vector yielded about 5×10^2 and 10^4 FFU/pmol of DNA in the absence and presence of EGF, respectively. Data represent averages of at least four independent experiments performed in duplicate. (B and C) EGF- and PDGF-BB-stimulated DNA synthesis in NIH-EGFR/*erb*B-2 and NIH-EGFR cells. Mass cell populations of NIH-EGFR/*erb*B-2 and NIH-EGFR cells were obtained by selection in a medium containing mycophenolic acid. Scatchard analysis of [^{125}I]EGF binding assays revealed the presence of two classes of receptors with affinities in the range of 10^{-9} M (low-affinity binding sites) and 10^{-10} M (high-affinity binding sites) in both cell lines. The total number of receptors was 1.6×10^6 and 1.5×10^6 receptors per cell for EGFR/*erb*B-2 and EGFR, respectively. Confluent cells were serum starved in Dulbecco's modified Eagle's medium supplemented with transferrin (5 μg/ml) and selenium (10 nM) for 72 h and then stimulated for 22 h with either 1% calf serum or EGF (B) or PDGF-BB (C) at the indicated concentrations, in the presence of 4 μCi of [*methyl*-^{3}H]thymidine per well. Data are expressed as percent maximal stimulation obtained in 1% calf serum according to the formula: [(cpm with EGF or PDGF) − (background cpm)]/[(cpm with 1% calf serum) − (background cpm)] × 100. (B) Symbols: ○, NIH-EGFR plus EGF; ●, NIH-EGFR/*erb*B-2 plus EGF. (C) Symbols: ○, NIH-EGFR plus PDGF-BB; ●, NIH-EGFR/*erb*B-2 plus PDGF-BB. Results are typical and representative of at least four independent experiments.

PDGFR. We next analyzed the ability of the EGFR/*erb*B-2 chimeric molecule to phosphorylate cellular proteins on tyrosine residues. In the first series of experiments, we compared PTyr-containing proteins in NIH-*erb*B-2 and NIH-EGFR/*erb*B-2 transfectants. As shown in Fig. 2A, extracts from both NIH/*erb*B-2 and NIH-EGFR/*erb*B-2 transfectants contained a prominent 185-kDa species detected by anti-PTyr antibodies. These bands corresponded to the *erb*B-2 and EGFR/*erb*B-2 185-kDa species recognized in the same extracts by peptide antisera directed against the tyrosine kinase (M1 antibody) or COOH-terminal (M6 antibody) region of the *erb*B-2 molecule (Fig. 2A and B). Of note, the EGFR/*erb*B-2 chimera displayed a basal level of tyrosine phosphorylation, consistent with the low but detectable transforming activity of this chimera in the absence of added EGF (Fig. 2C).

Additional PTyr-containing proteins were also detected in extracts from NIH-*erb*B-2 and NIH-EGFR/*erb*B-2 transfectants (Fig. 2A). A major PTyr-containing species (~170 kDa), migrating close to gp185$^{erbB\text{-}2}$ and gp185$^{EGFR/erbB\text{-}2}$, likely represents a precursor or a partial COOH-terminal degradation product of these proteins and was occasionally detected in direct immunoblotting with the M1 antibody (data not shown). Of note, the high-molecular-mass region of the gel (100 to 200 kDa) contained a characteristic triplet of putative substrates (~135, ~115, and ~100 kDa, indicated with arrowheads in Fig. 2A). This pattern of PTyr-containing proteins appeared to be identical in NIH-*erb*B-2 transfectants and NIH-EGFR/*erb*B-2 cells stimulated with EGF (Fig. 2A). Moreover, these proteins were not detectable in direct immunoblotting with the two *erb*B-2-specific antipeptide sera M1 and M6 (Fig. 2B), supporting the notion that the

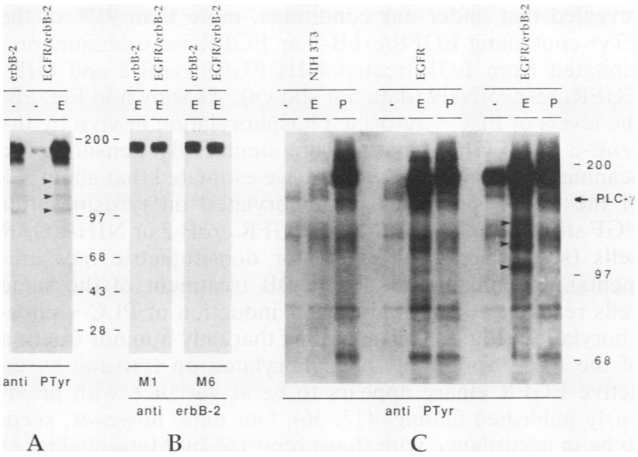

FIG. 2. Tyrosine phosphorylation of cellular proteins in NIH 3T3 cells transfected with LTR-EGFR/*erb*B-2, LTR-*erb*B-2, or LTR-EGFR. The two mass cell populations of NIH-EGFR/*erb*B-2 and NIH-EGFR described in the legend to Fig. 1 and a marker-selected mass cell population of NIH-*erb*B-2 from the same transfection experiment were used. Cells were either mock treated (—) or treated with EGF (100 ng/ml) (E) or PDGF-BB (100 ng/ml) (P) for 10 min at 37°C before lysis. Total cellular proteins (200 μg) were fractionated by electrophoresis and subjected to immunoblot analysis. (A) Immunodetection was carried out with the anti-PTyr antibody. Preclearing of the lysates with M6 serum but not with normal rabbit serum or with M6 preabsorbed with the specific peptide selectively removed the 185-kDa proteins recognized by the anti-PTyr antibody (data not shown). Solid arrowheads indicate the ~135-, ~115-, and ~100-kDa putative substrates. (B) Immunodetection was performed with the *erb*B-2 antipeptide sera M1 and M6 described in Materials and Methods. (C) Immunodetection was performed with the anti-PTyr antibody. The autoradiogram is overexposed to reveal the presence of low-abundance PTyr-containing proteins. Solid arrowheads indicate the ~135-, ~115-, and ~100-kDa putative substrates. Molecular mass markers are shown in kilodaltons, the position of tyrosine-phosphorylated PLC-γ is also indicated. Results are typical and representative of at least three independent experiments.

~135-, ~115-, and ~100-kDa species represent "true" substrates rather than degradation products of *erb*B-2. On the basis of this biological and biochemical evidence, we concluded that the EGFR/*erb*B-2 chimera was able to transduce an EGF-mediated signal via the *erb*B-2-specific mitogenic signaling pathway.

We next compared tyrosine phosphorylation of putative substrates by the *erb*B-2 and EGFR kinases. As shown in Fig. 2C, there were both quantitative and qualitative differences in the pattern of PTyr-containing proteins observed upon EGF triggering of the two cell lines. In particular, species of ~135 and ~100 kDa which were tyrosine phosphorylated upon activation of the *erb*B-2 kinase did not appear to be substrates for the EGFR (Fig. 2C). The immunoblot presented in Fig. 2C was obtained from a longer gel run than that shown in Fig. 2A. Under these conditions, the ~115-kDa band resolved as a doublet, which seemed to be a substrate for both active EGFR and *erb*B-2 kinase. The lower band of the doublet (indicated in Fig. 2C by the second black arrowhead from the top) appeared to be more intensely phosphorylated by EGFR/*erb*B-2 than by EGFR. At present, we do not know whether this difference is merely quantitative or reflects the comigration of a distinct *erb*B-2-specific substrate with the ~115-kDa doublet, which is a common substrate for EGFR and *erb*B-2. Other differences affecting minor tyrosine-phosphorylated species were also detected in the 80- to 85-kDa region, between NIH-EGFR and NIH-EGFR/*erb*B-2 cells treated with EGF (Fig. 2C). All these observations support the concept that *erb*B-2 and EGFR signal through mitogenic pathways which are at least in part distinct (7).

PDGF-BB triggering induced tyrosine phosphorylation of a similar subset of substrates in NIH 3T3, NIH-EGFR, and NIH-EGFR/*erb*B-2 cells (Fig. 2C). In the case of PDGF-BB-triggered cells, we were able to demonstrate that a major PTyr-containing band of ~150 kDa (Fig. 2C) comigrated with authentic PLC-γ, as expected. This band did not seem to be a major substrate for the active EGFR or *erb*B-2 kinase (Fig. 2C; see below for a more detailed discussion). Of interest, the pattern of PTyr-containing proteins detected in PDGF-BB-triggered cells was conspicuously different from that observed in EGF-triggered NIH-EGFR/*erb*B-2 cells. Thus, the signaling pathways mediating the action of *erb*B-2 and PDGFR are likely to be at least partly divergent as well.

Coimmunoprecipitation and tyrosine phosphorylation of PLC-γ by *erb*B-2 and EGFR kinases. As an approach to investigating the biochemical basis for the greater mitogenic potency of the *erb*B-2 kinase than of EGFR in NIH 3T3 cells, we compared their ability to couple with known pathways implicated in mitogenic signal transduction. One such pathway, leading to increased PIP_2 breakdown, is thought to be initiated by tyrosine phosphorylation of PLC-γ by receptor tyrosine kinases. As shown in Fig. 3A, EGF stimulation of either NIH-EGFR/*erb*B-2 or NIH-EGFR induced tyrosine phosphorylation of PLC-γ. In addition, NIH-*erb*B-2 cells showed a higher steady-state content of PTyr-containing PLC-γ than mock-transfected NIH 3T3 cells (data not shown), further proving that PLC-γ is a substrate for the *erb*B-2 kinase. Of note, in NIH-EGFR and NIH-EGFR/*erb*B-2 cells at comparable levels of receptor expression and ligand stimulation, the extent of PLC-γ tyrosine phosphorylation was comparable (Fig. 3A, left panel). Since no appreciable differences were detected in steady-state levels of PLC-γ in these cells (Fig. 3A, central panel) and quantitative immunoprecipitation was achieved under our conditions of analysis (data not shown), we concluded that the *erb*B-2 and EGFR kinases were capable of phosphorylating PLC-γ with comparable efficiency.

Previous studies (14, 17, 18) have demonstrated coimmunoprecipitation of PLC-γ with PDGFRs or EGFRs. The specificity of this to ligand-stimulated receptors has indicated that PLC-γ phosphorylation is the result of direct interaction with the activated receptor tyrosine kinases. As shown in Fig. 3A, left panel, in addition to PLC-γ itself, a second tyrosine-phosphorylated protein was detected in cell lysates obtained from either EGF-stimulated NIH-EGFR/*erb*B-2 or NIH-EGFR following immunoprecipitation with anti-PLC-γ antibodies. The relative molecular masses of these proteins were 185 and 170 kDa, respectively, consistent with the respective sizes of the EGFR/*erb*B-2 chimera and EGFR. Indeed, immunoblot analysis of anti-PLC-γ immunoprecipitates with *erb*B-2- or EGFR-specific antibodies (Fig. 3A, right panel) identified the 185- and 170-kDa bands as EGFR/*erb*B-2 and EGFR, respectively, indicating a physical association between PLC-γ and the *erb*B-2 kinase in vivo.

To estimate the percentage of PLC-γ molecules tyrosine phosphorylated upon activation of the *erb*B-2 and EGFR kinases, cell lysates from NIH-EGFR/*erb*B-2 and NIH-EGFR were subjected to quantitative immunoprecipitation

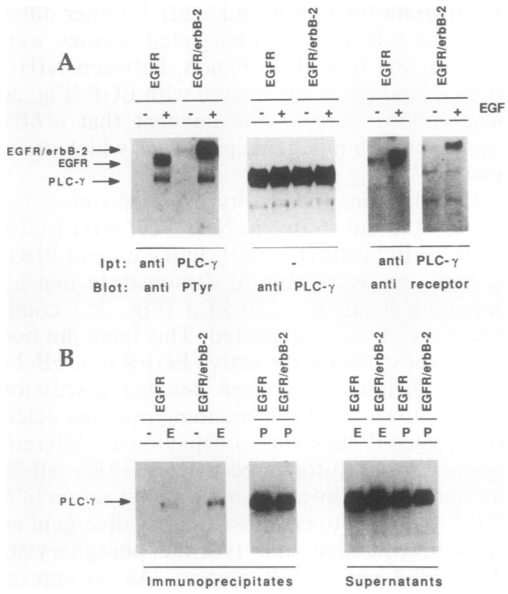

FIG. 3. In vivo tyrosine phosphorylation of PLC-γ by EGFR/*erb*B-2 and EGFR. The two marker-selected mass cell populations of NIH-EGFR/*erb*B-2 and NIH-EGFR described in the legend to Fig. 1 were used. Cells were treated with EGF or PDGF-BB at 37°C for 10 min where indicated. (A) Tyrosine phosphorylation and coimmunoprecipitation of PLC-γ with EGFR and EGFR/*erb*B-2. Cells were either treated with EGF (100 ng/ml, lanes +) or mock treated (lanes −). (Left panel) Total cellular proteins (1.0 mg) were immunoprecipitated (Ipt) with a mixture of six MAbs against PLC-γ (32) and analyzed by immunoblot with an anti-PTyr antibody. (Central panel) Total cellular proteins (50 μg) were fractionated on a 4 to 20% acrylamide gradient gel and analyzed by immunoblot with the anti-PLC-γ antibodies. (Right panel) Total cellular proteins (1.0 mg) were immunoprecipitated with the anti-PLC-γ antibodies and analyzed by immunoblot with either the E7 (anti-EGFR) or the M6 (anti-*erb*B-2) antibody. (B) Stoichiometry of phosphorylation of PLC-γ by EGFR/*erb*B-2, EGFR, and PDGFR. Cells were either mock treated (−) or treated with EGF (E) or PDGF-BB (P). Total cell lysates (1.0 mg) were immunoprecipitated with an excess of the anti-PTyr antibody. Specific immunoprecipitates were then analyzed by immunoblot with the anti-PLC-γ antibodies (left panel). Supernatants from the immunoprecipitation reactions (1/10 of the reaction mixture, corresponding to 100 μg of total cellular proteins) were also analyzed by immunoblot with the anti-PLC-γ antibodies (right panel). The results presented here were obtained with the affinity-purified anti-PTyr polyclonal antibody described in Materials and Methods. Identical results were obtained with two commercially available MAbs (PY20 and an anti-PTyr MAb) (data not shown). Densitometric scans of the autoradiograms in panel B were performed on several exposures taken in the linear range of signal intensity. Relative signal intensities were calculated on the basis of the areas of the individual peaks, measured in optical density times millimeters, and converted to arbitrary units after normalization for the amount of protein loaded. Molecular mass markers are indicated in kilodaltons. Comparable results were obtained in four independent experiments.

with excess anti-PTyr antibodies; the immunoprecipitates as well as the supernatants were blotted with anti-PLC-γ antibodies. EGF was added at a concentration of 300 ng/ml (~50 nM) for 5 min at 37°C; this concentration was determined in experiments which showed that optimal PLC-γ tyrosine phosphorylation by both EGFR/*erb*B-2 and EGFR occurred under these conditions (data not shown). A series of control reactions involving sequential anti-PTyr immunoprecipitation and blotting with anti-EGFR or anti-*erb*B-2 antibodies revealed that under our conditions, more than 95% of the PTyr-containing EGFR/*erb*B-2 or EGFR were immunoprecipitated from EGF-treated NIH-EGFR/*erb*B-2 and NIH-EGFR, respectively (data not shown). As shown in Fig. 3B, the levels of PLC-γ tyrosine phosphorylation in vivo by the *erb*B-2 and EGFR kinases were similar. By densitometric scanning of the autoradiograms, we estimated that about 1% of the PLC-γ pool was phosphorylated on tyrosine after EGF stimulation of either NIH-EGFR/*erb*B-2 or NIH-EGFR cells (see legend to Fig. 3B for densitometric measurements). In comparison, PDGF-BB treatment of the same cells resulted in a 15-fold-greater induction of PLC-γ phosphorylation (Fig. 3B). The finding that only a minor fraction of the PLC-γ pool was phosphorylated on tyrosine by an active EGFR kinase appears to be at variance with previously published findings (17, 36). Our data, however, seem to be in accordance with those reported by Meisenhelder et al. (18), who detected a lower stoichiometry of PLC-γ phosphorylation by EGFR than by PDGFR.

Phosphopeptide maps of PLC-γ from EGF- and PDGF-treated NIH-EGFR/*erb*B-2 and NIH-EGFR. Two-dimensional analysis of phosphopeptides was undertaken to compare the patterns of PLC-γ phosphorylations induced by activation of the *erb*B-2 and EGFR kinases. Two peptides containing phosphoserine (peptides 1 and 2 in Fig. 4A) were prominent before stimulation with growth factors. Upon treatment of NIH-EGFR cells with PDGF-BB, three new peptides containing PTyr (peptides a, b, and c in Fig. 4D) appeared. These maps closely resembled those previously described for PLC-γ from NIH 3T3 cells treated with PDGF (18, 22). EGF treatment of NIH-EGFR/*erb*B-2 (Fig. 4B) and NIH-EGFR (Fig. 4C) cells also produced the three new PTyr-containing peptides. However, the relative intensity of the PTyr-containing to the phosphoserine-containing peptides was significantly lower with the EGF-treated cells than with the PDGF-BB-treated cells. No significant differences could be found in the relative intensity of signals between EGF-treated NIH-EGFR/*erb*B-2 and NIH-EGFR.

Coupling of *erb*B-2 and EGFR kinases with the inositol lipid second-messenger pathway. Several lines of evidence argue that PLC-γ tyrosine phosphorylation results in the activation of its enzymatic activity and increased PIP_2 breakdown (see, for example, reference 18 and references therein). To examine the effects of *erb*B-2 kinase activation on phosphatidylinositol turnover, we measured the formation of inositol phosphates in cells labeled with [*myo*-^{3}H]inositol. Table 1 shows that activation of the *erb*B-2 kinase induced the formation of ^{3}H-inositol phosphates in NIH-EGFR/*erb*B-2 cells. However, the magnitude of this effect was relatively small, with only a twofold increase under our experimental conditions. Moreover, comparable increases were observed in both NIH-EGFR/*erb*B-2 and NIH-EGFR cells treated with EGF, consistent with the similar low efficiency of PLC-γ phosphorylation (Table 1). In contrast, PDGF-BB stimulation of the same cell lines resulted in an 8- to 10-fold increase in ^{3}H-inositol phosphates. These findings were also consistent with the greater efficiency of PLC-γ tyrosine phosphorylation in response to PDGFR activation in these cells.

Tyrosine phosphorylation of GAP by *erb*B-2 and EGFR kinases. Recent evidence has implicated GAP as an early substrate for the PDGFR and EGFR kinases (9, 12, 19). To test whether GAP is a substrate for the *erb*B-2 kinase, we analyzed the effects of EGF triggering of NIH-EGFR/*erb*B-2 cells on GAP tyrosine phosphorylation. To this end, total cellular proteins from NIH-EGFR/*erb*B-2, NIH-EGFR, and

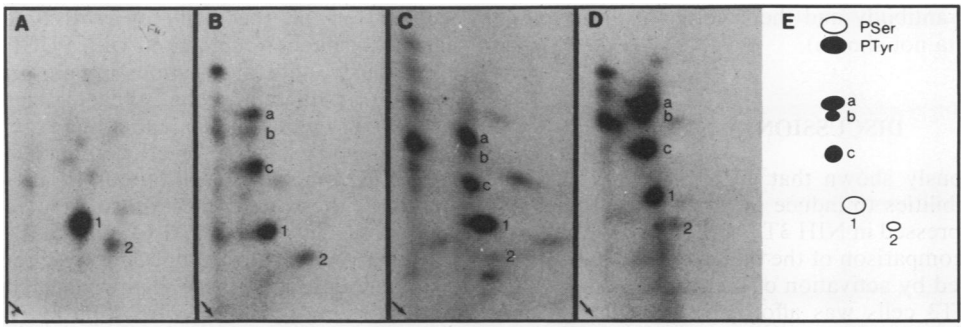

FIG. 4. Phosphopeptide maps of PLC-γ in EGFR/*erb*B-2 and EGFR transfectants after growth factor stimulation. Tryptic digests were prepared from ^{32}P-labeled, immunoprecipitated PLC-γ from unstimulated NIH-EGFR cells or from NIH-EGFR and NIH-EGFR/*erb*B-2 cells treated for 5 min at 37°C with either EGF (100 ng/ml) or PDGF-BB (100 ng/ml). Peptides were resolved in two dimensions on cellulose thin-layer plates by electrophoresis (horizontal dimension; anode on the left) and chromatography (vertical dimension), as described in Materials and Methods. The following samples were analyzed (the values in parentheses indicate the number of Cerenkov counts per minute loaded and the time that the gel was exposed to XAR film at −70°C with an intensifying screen): (A) untreated NIH-EGFR (150 cpm, 9 days); (B) EGF-treated NIH-EGFR/*erb*B-2 (220 cpm, 7 days); (C) EGF-treated NIH-EGFR cells (230 cpm, 7 days); and (D) PDGF-treated NIH-EGFR cells (280 cpm, 6 days). (E) Schematic representation of phosphopeptides in which solid and open circles represent PTyr-containing and phosphoserine (PSer)-containing peptides, respectively. Origins are indicated by arrows. Peptides 1, 2, a, b, and c are indicated.

mock-transfected NIH 3T3 cells treated with EGF or PDGF-BB were quantitatively immunoprecipitated with an anti-PTyr antibody and the specific immunoprecipitates were subjected to immunoblotting with anti-GAP serum 637 (see Materials and Methods). As shown in Fig. 5, immunoprecipitation with an anti-PTyr antibody led to recovery of a minute amount of GAP in lysates of NIH-EGFR/*erb*B-2 cells stimulated with EGF. Moreover, under identical conditions of ligand stimulation, the levels of anti-PTyr-recoverable GAP were comparable in EGF-stimulated NIH-EGFR/*erb*B-2 and in NIH-EGFR. Since there were no appreciable differences in the steady-state levels of GAP in these cell lines (Fig. 5B), we concluded that the *erb*B-2 and EGFR kinases were able to phosphorylate GAP with a comparable low efficiency.

Conversely, upon PDGF-BB triggering of the same cells, at least 30-fold higher levels of GAP were recovered by anti-PTyr immunoprecipitation (Fig. 5A). Under these latter conditions, ~30% of the GAP pool is tyrosine phosphorylated (18a); therefore, we estimated that a maximally stimulated *erb*B-2 kinase is able to induce tyrosine phosphorylation of ≤1% of the GAP pool. Similar results were obtained when total cellular lysates were first immunoprecipitated

TABLE 1. Effects of EGF and PDGF-BB on inositol phosphate formation in NIH 3T3, NIH-EGFR, and NIH-EGFR/*erb*B-2 cells[a]

Treatment	Fold stimulation (mean ± SE)		
	NIH 3T3	NIH-EGFR	NIH-EGFR/*erb*B-2
No addition	1.00 ± 0.01	1.00 ± 0.02	1.00 ± 0.01
EGF	1.05 ± 0.04	2.24 ± 0.07	2.11 ± 0.08
PDGF	9.36 ± 0.62	8.82 ± 0.45	7.62 ± 0.61

[a] Subconfluent cultures of NIH 3T3, NIH-EGFR, and NIH-EGFR/*erb*B-2 cells were labeled with [*myo*-^{3}H]inositol and stimulated with EGF or PDGF for 30 min, as indicated in Materials and Methods. Inositol phosphates were analyzed by anion-exchange chromatography. Results were normalized for the value of total inositol-containing phospholipids and are expressed as fold stimulation over control (unstimulated) values for each cell line; values represent means ± SE (n = 4). The basal inositol phosphate level of a representative experiment in NIH-EGFR/*erb*B-2 cells was 11,048 ± 1,209 cpm (IP1, 9,373 cpm; IP2, 1,507 cpm; IP3, 168 cpm). After stimulation with EGF for 30 min, the levels were 20,705 (IP1), 2,422 (IP2), and 385 (IP3) cpm (total, 23,512 ± 964 cpm). The basal level for NIH-EGFR in the same experiment was 9,380 ± 704 cpm (IP1, 7,967 cpm; IP2, 1,281 cpm; IP3, 132 cpm). The preponderance of inositol monophosphates after 30 min of stimulation with EGF is probably due to the rapid dephosphorylation of calcium-mobilizing inositol phosphates which were formed during the initial phase of stimulation.

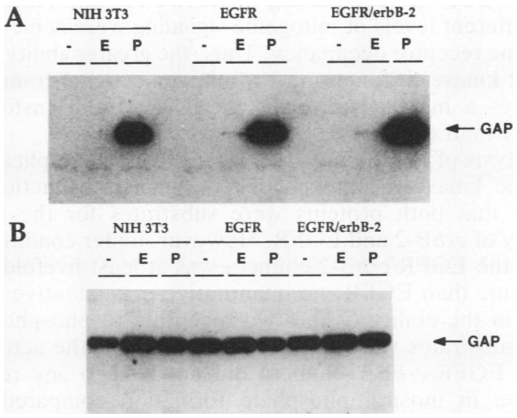

FIG. 5. In vivo tyrosine phosphorylation of GAP by EGFR/*erb*B-2, EGFR, and PDGFR. The two marker-selected mass cell populations of NIH-EGFR/*erb*B-2 and NIH-EGFR indicated in the legend to Fig. 1 were used. Control NIH 3T3 cells transfected with the vector alone (LTR-2 vector [5]) and marker-selected in mycophenolic acid were also used. Cells were either mock treated (—) or treated with EGF (100 ng/ml) (E) or PDGF-BB (100 ng/ml) (P) at 37°C for 10 min. (A) Total cellular proteins (1.0 mg) were immunoprecipitated with an excess of the anti-PTyr antibody and analyzed by immunoblot with an anti-GAP antibody. The results presented here were obtained with the affinity-purified anti-PTyr polyclonal antibody described in Materials and Methods. Identical results were obtained with commercially available MAbs. (B) Total cellular proteins (50 μg) were analyzed by immunoblot with the anti-GAP antibody. Densitometric scans of the autoradiograms were performed on several exposures taken in the linear range of signal intensity. Relative signal intensities were calculated on the basis of the areas of the individual peaks, measured in optical density times millimeters, and converted to arbitrary units after normalization for the amount of protein loaded. The autoradiogram presented in panel A was exposed for 96 h to show the faint GAP-specific band in NIH-EGFR and NIH-EGFR/*erb*B-2 cells. Molecular mass markers are indicated in kilodaltons. Comparable results were obtained in three independent experiments.

with an anti-GAP antibody and then blotted with an anti-PTyr antibody (data not shown).

DISCUSSION

We have previously shown that gp185^{erbB-2} and EGFR display different abilities to induce the transformed phenotype when overexpressed in NIH 3T3 fibroblasts (4, 5, 7). In this study, direct comparison of the biological and biochemical events triggered by activation of the *erb*B-2 and EGFR kinases in NIH 3T3 cells was afforded by the use of an EGFR/*erb*B-2 chimera. Since maximal activation of both EGFR/*erb*B-2 and EGFR was induced by EGF binding, it was possible to study mitogenic signaling under conditions in which the cellular responses to EGF were solely dependent on the coupling of either kinase with its own signaling pathway(s). In addition, cell lines were obtained which expressed similar levels of either EGFR/*erb*B-2 or EGFR, allowing rigorous quantitative analysis.

Under these conditions, the EGFR/*erb*B-2 chimera was approximately 100-fold more efficient at inducing cell transformation than the EGFR when activated by EGF. In addition, we demonstrated that the EGFR/*erb*B-2 chimera conferred upon the recipient cells increased responsiveness to EGF compared with EGFR. The half-maximal mitogenic stimulation in response to EGF was at least fivefold higher in NIH-EGFR/*erb*B-2 than in NIH-EGFR cells. However, the ED_{50} of EGF was comparable in the two cell lines, indicating that different levels of mitogenic signaling were achieved by the same receptor occupancy. Thus, the greater ability of the *erb*B-2 kinase to function as a mitogenic signal transducer provides a mechanistic basis for its greater transforming activity than the EGFR.

Analysis of PLC-γ and GAP, two substrates implicated in tyrosine kinase receptor-mediated signal transduction, revealed that both proteins were substrates for the kinase activity of *erb*B-2 and EGFR. However, under conditions in which the EGFR/*erb*B-2 chimera was at least fivefold more mitogenic than EGFR, no quantitative or qualitative differences in the ability of the two receptors to phosphorylate these substrates were observed. In addition, the activation of the EGFR/*erb*B-2 chimera did not lead to any relative increase in inositol phosphate formation compared with EGFR. Thus, our results demonstrate that the stronger mitogenic potency of the *erb*B-2 kinase than of the EGFR cannot be ascribed to either enhanced PIP_2 breakdown or putative signaling through the p21^{ras}/GAP pathway.

Under our experimental conditions, only a minor fraction of the PLC-γ and GAP pools were phosphorylated on tyrosine residues by the activated *erb*B-2 kinase in NIH-EGFR/*erb*B-2 cells. Conversely, in the same cell line, activated PDGFRs were capable of phosphorylating about 15 to 20% of PLC-γ, a figure lower than but on the same order of magnitude as reported previously (18, 40), and about 30% of the GAP pool (18a). Thus, despite the higher levels of expression (1.5×10^6 EGFRs/*erb*B-2 per cell versus 1.3×10^5 PDGFRs/cell in NIH-EGFR/*erb*B-2 cells), the *erb*B-2 kinase was still about 10- to 15-fold less efficient than PDGFR in phosphorylating PLC-γ and inducing turnover of inositol phospholipids and at least 30-fold less efficient in phosphorylating GAP. In NIH-EGFR/*erb*B-2 cells, however, EGF and PDGF-BB were able to induce a similar maximal mitogenic response, indicating that activation of pathways initiated by PLC-γ tyrosine phosphorylation and PIP_2 breakdown or by p21^{ras}/GAP signaling are unlikely to account for the specificity of *erb*B-2-mediated mitogenic signal transduction, compared with PDGFR.

Obviously, several questions remain unanswered regarding the transduction of the mitogenic signal by the *erb*B-2 kinase. Our findings indicate that there are differences in the repertoire of postreceptor effector molecules activated by *erb*B-2 in comparison with either EGFR or PDGFR. Furthermore, these differences must involve pathways other than those activated by PLC-γ or GAP phosphorylation. However, our results do not address directly whether activation of either of these pathways is necessary for the mitogenic action of the *erb*B-2 kinase. The low stoichiometry of tyrosine phosphorylation of PLC-γ and GAP by an active EGFR/*erb*B-2 seems to argue against this possibility. In this regard, our results with the *erb*B-2 kinase bear resemblance to those obtained with the colony-stimulating factor 1 (CSF-1) receptor. In NIH 3T3 cells expressing the CSF-1 receptor, CSF-1 stimulation does not result in PLC-γ tyrosine phosphorylation (8) and causes poor tyrosine phosphorylation of GAP (27). Thus, the mitogenic response activated by certain growth factor receptors, including *erb*B-2, might not obligatorily involve signaling through these two pathways. More direct evidence on this issue is likely to come from investigations of whether microinjection of antibodies directed against PLC-γ, GAP, and p21^{ras} can inhibit *erb*B-2-induced mitogenesis.

Our results also leave open the question of the molecular nature of a putative *erb*B-2-specific mitogenic pathway. Other second messengers, such as phosphatidylinositol 3-kinase (2, 13, 28, 38) and c-*raf* (20, 21), have been implicated as early substrates for receptor tyrosine kinases. However, our unpublished observations indicate that neither of these pathways can efficiently couple with the *erb*B-2 kinase. In fact, after EGF stimulation of NIH-EGFR/*erb*B-2, we have been unable to show either tyrosine phosphorylation of c-*raf* (9a) or activation of phosphatidylinositol 3-kinase (11a). A potential approach to the characterization of an *erb*B-2-specific mitogenic pathway comes from our observations that activation of the *erb*B-2 kinase caused tyrosine phosphorylation of a subset of putative substrates different from that observed with either the EGFR or PDGFR. In particular, a ~135-kDa and a ~100-kDa species were efficiently tyrosine-phosphorylated by active gp185^{erbB-2} and the EGFR/*erb*B-2 chimera but not by EGFR or PDGFR. Further investigations will be needed to molecularly characterize these species in order to evaluate their possible role in mediating the mitogenic actions of gp185^{erbB-2}.

ACKNOWLEDGMENTS

We are indebted to S. A. Aaronson for continuous support and encouragement and for critically reviewing the manuscript. We also thank M. Marshall for providing the anti-GAP antibody and D. P. Bottaro and M. Ruggiero for helpful discussions and suggestions. The expert technical assistance of M. Pangelinan is also acknowledge.

F. Fazioli is the recipient of a fellowship from the Associazione Italiana per la Ricerca sul Cancro (AIRC).

REFERENCES

1. **Bargmann, C. I., M. C. Hung, and R. A. Weinberg.** 1986. The *neu* oncogene encodes an epidermal growth factor receptor-related protein. Nature (London) **319**:226–230.
2. **Coughlin, S. R., J. A. Escobedo, and L. T. Williams.** 1989. Role of phosphatidylinositol kinase in PDGF receptor signal transduction. Science **243**:1191–1194.
3. **Coussens, L., F. T. Yang, Y. C. Liao, E. Chen, A. Gray, J. McGrath, P. H. Seeburg, T. A. Libermann, J. Schlessinger, U.**

Francke, A. Levinson, and A. Ullrich. 1985. Tyrosine kinase receptor with extensive homology to EGF receptor shares chromosomal location with *neu* oncogene. Science **230**:1132–1139.

4. **Di Fiore, P. P., J. H. Pierce, T. P. Fleming, R. Hazan, A. Ullrich, C. R. King, J. Schlessinger, and S. A. Aaronson.** 1987. Overexpression of the human EGF receptor confers an EGF-dependent transformed phenotype to NIH 3T3 cells. Cell **51**:1063–1070.
5. **Di Fiore, P. P., J. H. Pierce, M. H. Kraus, O. Segatto, C. R. King, and S. A. Aaronson.** 1987. *erb*B-2 is a potent oncogene when overexpressed in NIH/3T3 cells. Science **237**:178–182.
6. **Di Fiore, P. P., O. Segatto, F. Lonardo, F. Fazioli, J. H. Pierce, and S. A. Aaronson.** 1990. The carboxy-terminal domains of *erb*B-2 and epidermal growth factor receptor exert different regulatory effects on intrinsic receptor tyrosine kinase function and transforming activity. Mol. Cell. Biol. **10**:2749–2756.
7. **Di Fiore, P. P., O. Segatto, W. G. Taylor, S. A. Aaronson, and J. H. Pierce.** 1990. EGF receptor and *erb*B-2 tyrosine kinase domains confer cell specificity for mitogenic signaling. Science **248**:79–83.
8. **Downing, J. R., B. L. Margolis, A. Zilberstein, R. A. Ashmun, A. Ullrich, C. J. Sherr, and J. Schlessinger.** 1989. Phospolipase C-gamma, a substrate for PDGF receptor kinase, is not phosphorylated on tyrosine during the mitogenic response to CSF-1. EMBO J. **8**:3345–3350.
9. **Ellis, C., M. Moran, F. McCormick, and T. Pawson.** 1990. Phosphorylation of GAP and GAP-associated proteins by transforming and mitogenic tyrosine kinases. Nature (London) **343**: 377–381.

9a. **Fazioli, F., O. Segatto, A. Pfeifer, and P. P. Di Fiore.** Unpublished data.

10. **Graham, F. L., and A. J. Van der Eb.** 1973. A new technique for the assay of infectivity of human adenovirus 5 DNA. Virology **52**:456–467.
11. **Hunter, T., and B. M. Sefton.** 1980. Transforming gene product of Rous sarcoma virus phosphorylates tyrosine. Proc. Natl. Acad. Sci. USA **77**:1311–1315.

11a. **Kapeller, R., F. Fazioli, O. Segatto, and P. P. Di Fiore.** Unpublished data.

12. **Kaplan, D. R., D. K. Morrison, G. Wong, F. McCormick, and L. T. Williams.** 1990. PDGF beta-receptor stimulates tyrosine phosphorylation of GAP and association of GAP with a signaling complex. Cell **61**:125–133.
13. **Kazlauskas, A., and J. A. Cooper.** 1989. Autophosphorylation of the PDGF receptor in the kinase insert region regulates interactions with cell proteins. Cell **58**:1121–1133.
14. **Kumjian, D. A., M. I. Wahl, S. G. Rhee, and T. O. Daniel.** 1989. Platelet-derived growth factor (PDGF) binding promotes physical association of PDGF receptor with phospholipase C. Proc. Natl. Acad. Sci. USA **86**:8232–8236.
15. **Lee, J., T. J. Dull, I. Lax, J. Schlessinger, and A. Ullrich.** 1989. HER2 cytoplasmic domain generates normal mitogenic and transforming signals in a chimeric receptor. EMBO J. **8**:167–173.
16. **Lehväslaiho, H., L. Lehtola, L. Sistonen, and K. Alitalo.** 1989. A chimeric EGF-R-*neu* proto-oncogene allows EGF to regulate *neu* tyrosine kinase and cell transformation. EMBO J. **8**:159–166.

16a. **Lonardo, F., E. Di Marco, C. R. King, J. H. Pierce, O. Segatto, S. A. Aaronson, and P. P. Di Fiore.** 1990. The normal *erb*B-2 product is an atypical receptor-like tyrosine kinase with constitutive activity in the absence of ligand. New Biol. **2**:992–1003.

17. **Margolis, B., S. G. Rhee, S. Felder, M. Mervic, R. Lyall, A. Levitzki, A. Ullrich, A. Zilberstein, and J. Schlessinger.** 1989. EGF induces tyrosine phosphorylation of phospholipase C-II: a potential mechanism for EGF receptor signaling. Cell **57**:1101–1107.
18. **Meisenhelder, J., P. G. Suh, S. G. Rhee, and T. Hunter.** 1989. Phospholipase C-gamma is a substrate for the PDGF and EGF receptor protein-tyrosine kinases in vivo and in vitro. Cell **57**:1109–1122.

18a. **Molloy, C. J.** Unpublished data.

19. **Molloy, C. J., D. P. Bottaro, T. P. Fleming, M. S. Marshall, J. B. Gibbs, and S. A. Aaronson.** 1989. PDGF induction of tyrosine phosphorylation of GTPase activating protein. Nature (London) **342**:711–714.
20. **Morrison, D. K., D. R. Kaplan, J. A. Escobedo, U. R. Rapp, T. M. Roberts, and L. T. Williams.** 1989. Direct activation of the serine/threonine kinase activity of Raf-1 through tyrosine phosphorylation by the PDGF beta-receptor. Cell **58**:649–657.
21. **Morrison, D. K., D. R. Kaplan, U. Rapp, and T. M. Roberts.** 1988. Signal transduction from membrane to cytoplasm: growth factors and membrane-bound oncogene products increase Raf-1 phosphorylation and associated protein kinase activity. Proc. Natl. Acad. Sci. USA **85**:8855–8859.
22. **Morrison, D. K., D. R. Kaplan, S. G. Rhee, and L. T. Williams.** 1990. Platelet-derived growth factor (PDGF)-dependent association of phospholipase C-gamma with the PDGF receptor signalling complex. Mol. Cell. Biol. **10**:2359–2366.
23. **Mulcahy, L. S., M. R. Smith, and D. W. Stacey.** 1985. Requirement for *ras* proto-oncogene function during serum-stimulated growth of NIH 3T3 cells. Nature (London) **313**:241–243.
24. **Mulligan, R. C., and P. Berg.** 1981. Selection for animal cells that express the *Escherichia coli* gene coding for xanthine-guanine phosphoribosyltransferase. Proc. Natl. Acad. Sci. USA **78**:2072–2076.
25. **Pang, D. T., B. R. Sharma, and J. A. Shafer.** 1985. Purification of the catalytically active phosphorylated form of insulin receptor kinase by affinity chromatography with *O*-phosphotyrosyl-binding antibodies. Arch. Biochem. Biophys. **242**:176–186.
26. **Pierce, J. H., M. Ruggiero, T. P. Fleming, P. P. Di Fiore, J. S. Greenberger, L. Varticovski, J. Schlessinger, G. Rovera, and S. A. Aaronson.** 1988. Signal transduction through the EGF receptor transfected in IL-3-dependent hematopoietic cells. Science **239**:628–631.
27. **Reedijk, M., X. Liu, and T. Pawson.** 1990. Interactions of phosphatidylinositol kinase, GTPase-activating protein (GAP), and GAP-associated proteins with the colony-stimulating factor 1 receptor. Mol. Cell. Biol. **10**:5601–5608.
28. **Ruderman, N. B., R. Kapeller, M. F. White, and L. C. Cantley.** 1990. Activation of phosphatidylinositol 3-kinase by insulin. Proc. Natl. Acad. Sci. USA **87**:1411–1415.
29. **Ruggiero, M., S. K. Srivastava, T. P. Fleming, D. Ron, and A. Eva.** 1989. NIH3T3 fibroblasts transformed by the *dbl* oncogene show altered expression of bradykinin receptors: effect on inositol lipid turnover. Oncogene **4**:767–771.
30. **Segatto, O., F. Lonardo, J. H. Pierce, D. P. Bottaro, and P. P. Di Fiore.** 1990. The role of autophosphorylation in modulation of *erb*B-2 transforming function. New Biol. **2**:187–195.
31. **Segatto, O., C. R. King, J. H. Pierce, P. P. Di Fiore, and S. A. Aaronson.** 1988. Different structural alterations upregulate in vitro tyrosine kinase activity and transforming potency of the *erb*B-2 gene. Mol. Cell. Biol. **8**:5570–5574.
32. **Smith, M. R., Y. L. Liu, H. Kim, S. G. Rhee, and H. F. Kung.** 1990. Inhibition of serum- and *ras*-stimulated DNA synthesis by antibodies to phospholipase C. Science **247**:1074–1077.
33. **Smith, M. R., S. H. Ryu, P. G. Suh, S. G. Rhee, and H. F. Kung.** 1989. S-phase induction and transformation of quiescent NIH 3T3 cells by microinjection of phospholipase C. Proc. Natl. Acad. Sci. USA **86**:3659–3663.
34. **Stern, D. F., M. P. Kamps, and H. Cao.** 1988. Oncogenic activation of $p185^{neu}$ stimulates tyrosine phosphorylation in vivo. Mol. Cell. Biol. **8**:3969–3973.
35. **Suh, P. G., S. H. Ryu, W. C. Choi, K. Y. Lee, and S. G. Rhee.** 1988. Monoclonal antibodies to three phospholipase C isozymes from bovine brain. J. Biol. Chem. **263**:14497–14504.
36. **Todderud, G., M. I. Wahl, S. G. Rhee, and G. Carpenter.** 1990. Stimulation of phospholipase C-γ1 membrane association by epidermal growth factor. Science **249**:296–298.
37. **Ullrich, A., L. Coussens, J. S. Hayflick, T. J. Dull, A. Gray, A. W. Tam, J. Lee, Y. Yarden, T. A. Libermann, J. Schlessinger, J. Downward, E. L. V. Mayes, N. Whittle, M. D. Waterfield, and P. H. Seeburg.** 1984. Human epidermal growth factor receptor cDNA sequence and aberrant expression of the amplified gene in A431 epidermoid carcinoma cells. Nature (London) **309**:418–425.

38. **Varticovski, L., B. Druker, D. Morrison, L. Cantley, and T. Roberts.** 1989. The colony stimulating factor-1 receptor associates with and activates phosphatidylinositol-3 kinase. Nature (London) **342**:699–702.
39. **Wahl, M. I., S. Nishibe, J. W. Kim, H. Kim, S. G. Rhee, and G. Carpenter.** 1990. Identification of two epidermal growth factor-sensitive tyrosine phosphorylation sites of phospholipase C-gamma in intact HSC-1 cells. J. Biol. Chem. **265**:3944–3948.
40. **Wahl, M. I., N. E. Olashaw, S. Nishibe, S. G. Rhee, W. J. Pledger, and G. Carpenter.** 1989. Platelet-derived growth factor induces rapid and sustained tyrosine phosphorylation of phospholipase C-gamma in quiescent BALB/c 3T3 cells. Mol. Cell. Biol. **9**:2934–2943.
41. **Wigler, M., S. Silverstein, L. S. Lee, A. Pellicer, Y. C. Cheng, and R. Axel.** 1977. Transfer of purified herpes virus thymidine kinase gene to cultured mouse cells. Cell **11**:223–232.